Electronic Supplementary Material (ESI) for Journal of Materials Chemistry C

Supporting Information

Growth of n-type 3*C*-SiC Nanoneedles on Carbon Fabric: Toward Extremely Flexible Field Emission Devices

Xinni Zhang[1,2*], *Youqiang Chen*[1,3*], *Wei Liu*[2], *Weijiang Xue*[2], *Jiahao Li*[4] *and Zhipeng Xie*[2*]
[1] *College of Physics Science, Qingdao University, Qingdao, 266071, P.R. China.*
[2] *State Key Lab of New Ceramics and Fine Processing, Tsinghua University, Beijing, 100084, P.R. China.*
[3] *Department of Chemistry, Tsinghua University, Beijing, 100084, P. R. China.*
[4] *Advanced Materials Laboratory, Department of Materials Science and Engineering, Tsinghua University, Beijing, 100084, P. R. China.*

1. 3*C*-SiCNN GROWTH CONDITION, AND STRUCTURAL AND MORPHOLOGICAL CHARACTERIZATION

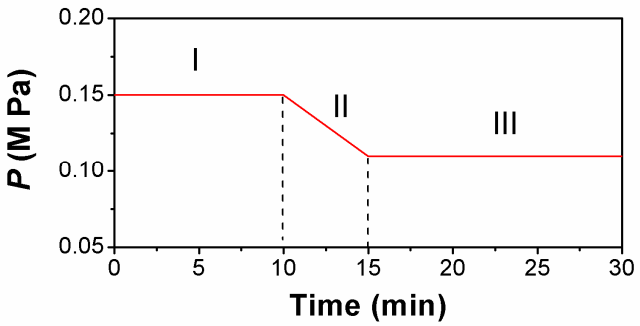

Figure S1. Schematic showing the Ar/N_2/reactant mixed gas pressure as a function of the reaction time during the SiCNN growth process. ***P*** is the mixed gas pressure in M Pa.

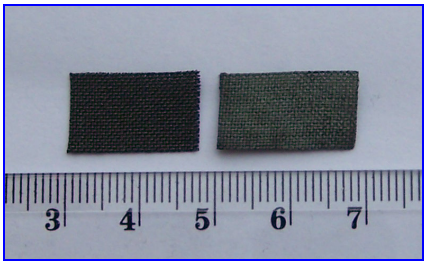

Figure S2. Macroscopic digital photos of the carbon fabric (a) before (left) and (b) after reaction (right).

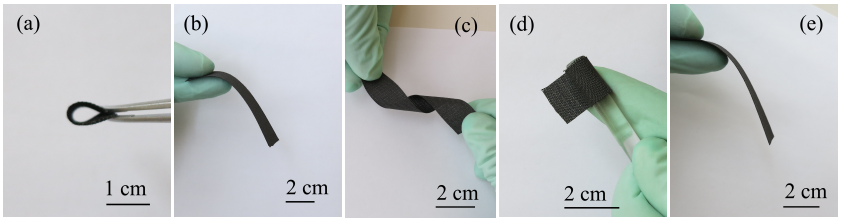

Figure S3. Digital photograph showing suspended and three different bending states of the carbon fabric after heat-treatment at 1700°C for 30 min: (a) folded (radius = ~ 0.3 cm), (b) suspended, (c) twisted, (d) rolled up (radius of the glass rod = ~ 0.35 cm) and (e) suspended again after being twisted and rolled up.

.

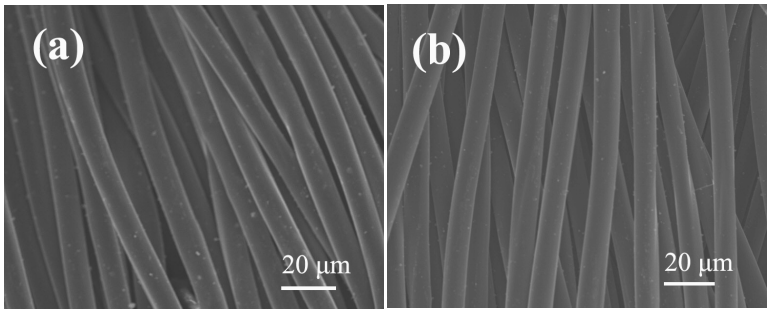

Figure S4. Typical SEM images of the carbon fabric (a) before and (b) after heat-treatment at 1700°C for 30 min, respectively.

Descriptions for Figure S3 and S4: To further verify the feasibility for our SiCNN fabrication method, an additional control experiment was performed on the pure CF after being thermally treated at very high temperature, 1700°C, for 30 min. The digital macrophotograph showed that the carbon fabric after a high-temperature heat treatment can also exhibit an impressive ultrahigh flexibility due to the heat treatment has no morphological destruction on the surfaces of fibers as seen in typical SEM images in Figure S4.

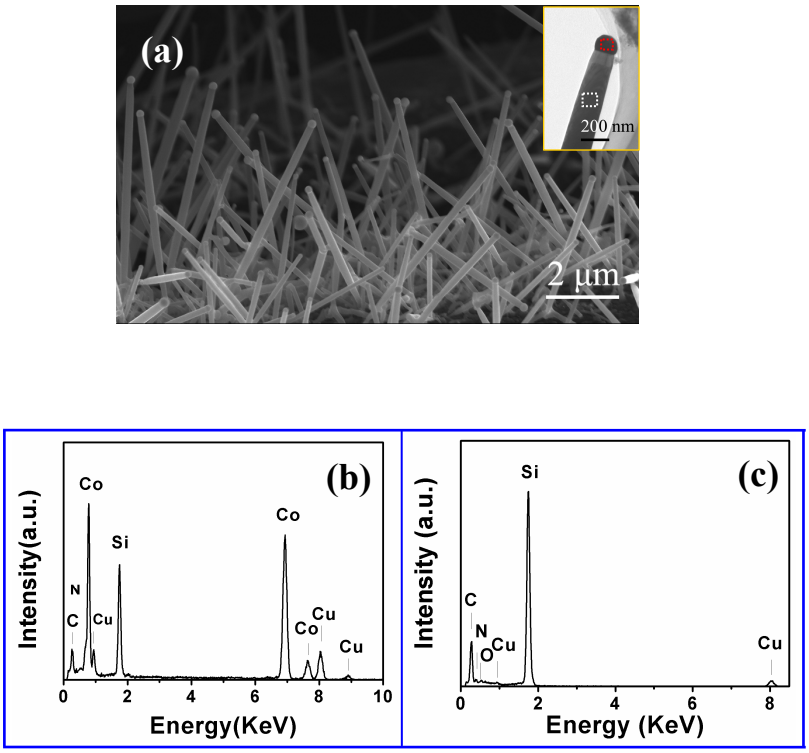

Figure S5. (a) Representative SEM images of 3*C*-SiCNNs obtained after 3 min heating time, showing catalytic droplets attached on their tips. Inset: A typical TEM image of a 3*C*-SiCNN with a catalytic droplet. (b) and (c): Corresponding EDS spectra taken from the catalytic droplet (marked with the dashed red rectangle) and SiCNN backbone (marked with the dashed white rectangle).

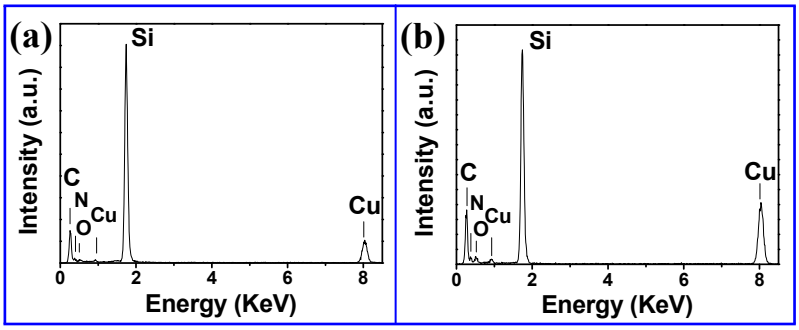

Figure S6. Representative EDS spectrums of samples, S2-N and S5-N, respectively.

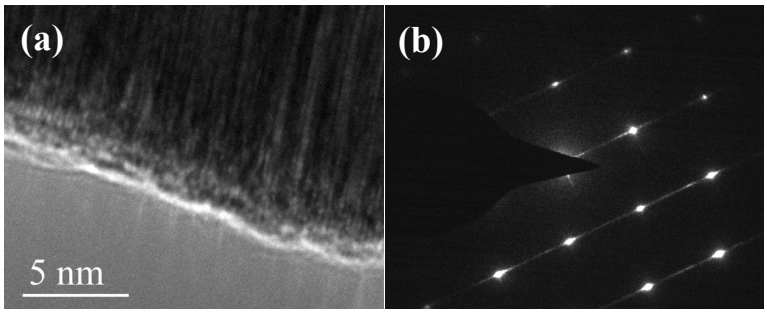

Figure S7. (a) A typical HRTEM image of the sample, S5-N. (b) Corresponding SAED pattern of S5-N.

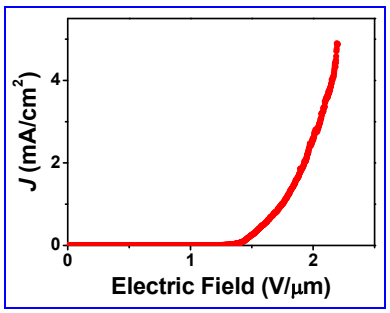

Figure S8. Field-emission current density versus electric field (*J*–*E*) for the structural analogy of S3-N for the control experiments (Note that this sample and S3-N were cut from the same functionalized carbon fabric).

2. GROWTH MECHANISM

Elevating the temperature in Ar followed by carbon reduction decomposed the

cobalt nitrate into cobalt nanoparticles, which then gradually formed catalyst Co-Si-C-O alloys after CO and SiO vapors transported to the catalysts on the carbon substrate.

$$4Co(NO_3)_3 = 2Co_2O_3 + 12NO_2 + 3O_2 \quad (1)$$

$$2Co_2O_3 + 3C = 4Co + CO_2 \quad (2)$$

The continuous dissolution of CO and SiO into the liquid catalyst droplets led to the supersaturation, within which overproduced SiC nucleated at the interface between the droplet and the carbon substrate.

$$SiO(v) + 3CO = SiC(s) + 2CO_2(v) \quad (3)$$

$$SiO(v) + 2C = SiC(s) + CO(v) \quad (4)$$

where (s) and (v) stand for solid and vapor states, respectively. Small droptes attached to the tips of SiCNNs could be clearly observed in the SEM and TEM images (Figure S5 (a)). The EDS analysis confirms that the droplet at the nanoneedle tips is composed of Co, C, Si, N and O, while the nanoneedle backbone only contains C, Si, O and N (Figure S5(b) and (c)), indicating that our SiCNN growth follows the conventional VLS growth mechanism. [1]

In the initial stage, a SiC nucleus would have a two-dimensional hexagonal shape with a (111) plane and six (110) peripheral planes to minimize the surface energy and specific line tension. As the precipitation proceeds, the nucleus tends to grow along {111}axial direction and push the droplet alloy away to maintain minimum total surface energy.[2]

Due to the very small size of nuclei, the droplet exhibits a large contact angle

that gives rise to an outward force to drive a lateral growth along the connective {111} planes and, thus, minimizes the lateral surface energy. This radial enlargement then immediately leads to the decrease of the interfacial contact angle. As such for the many SiC NWs the hexagonal cross-section often tapers inward near the NW bottom base creating an inverted pyramidal structure at the substrate-NW interface that actually does not favor the high-performance field emission. However, under our high-temperature heating conditions, the droplet underwent a continuous size reduction owing to droplet evaporation. Therefore, the taped SiCNNs with clear tiny tips that are tilted upward result since the growth of a nanowire was strictly confined within a catalyst-droplet.

REFERENCES

1 R. B. Wu, K. Zhou, J. Wei, Y. Z. Huang, F. Su, J. J. Chen and L. Y. Wang, *J. Phys. Chem. C*, 2012, **116**, 12940.
2 H. Wang, Z. Xie, W. Yang, J. Fang and L. An, *Cryst. Growth Des.,* 2008, **8**, 3893.